

Selective Adiabatic Refocusing Pulse Train for Nonlinear Phase Dispersion and Flip Angle Error Compensation

Z. Sun¹, and J. L. Zweier¹

¹Davis Heart & Lung Research Institute, The Ohio State University, Columbus, Ohio, United States

Introduction: Adiabatic full passage (AFP) pulses are well known for their immunity to the B_1 inhomogeneity [1], and have been applied in many areas of magnetic resonance spectroscopy (MRS) and MRI, such as signal sensitivity enhancement and sharp volume boundary definition [2-4]. However, the application of selective AFP refocusing pulses has been limited by the inherent nonlinear phase dispersion and off-resonance effect. To address this problem, extensive research work has been conducted for improving signal sensitivity [5-7]. Nonlinear phase dispersion produced by a selective 90° (HS1) pulse can be approximately expressed as $\varphi_1 = \pi v^2/a$, where v is the resonance frequency of spins and a is the frequency accelerator [5,7]. If the same pulse sweeps reversely, the nonlinear phase dispersion can be approximated as $\varphi_2 = -\varphi_1 = -\pi v^2/a$. Thus, the net nonlinear phase dispersion generated by two selective 90° (HS1) pulses with alternate frequency sweep (AFS) directions is zero. Due to the AFS mechanism of the two pulses, the off-resonance induced flip-angle error of the first 90° (HS1) pulse can be compensated by the second one with AFS. In this study, we designed and implemented an adiabatic refocusing pulse train that compensates the nonlinear phase dispersion and off-resonance induced flip-angle errors across the 3D volume. The AFS-AFP pulse train also excises spin-locking along the static field (B_0) direction.

Methods: The adiabatic pulse train consisted of two 90° HS1_R20 pulses (pulse length 4 ms, band width (BW) 4 kHz, $B_1(\text{max})$ 587 Hz, pulse power = 8 dB) for AFS spin flipping at the two ends of the pulse trains, and two low power HS1_R20 AFP pulses (pulse length = 4 ms, BW = 4 kHz, $B_1(\text{max})$ = 2.3 kHz, pulse power = 40 dB) for spin locking along the B_0 direction in the middle. The NMR-SIM from Bruker was used to model the flip-angle error compensation effect. After the 90° hermite excitation pulse (pulse length = 2 ms, BW = 2700 Hz), spin refocus was simulated with an initial magnetization components of $M_x(0) = M_y(0) = 1/\sqrt{2}$, $M_z(0) = 0$, for the RF offset (Ω) of 0, 250, 500, 750, and 1000 Hz, for both AFS-AFP and hermite refocusing pulses (pulse length = 1267 us, $B_1(\text{max})$ = 2.2 kHz). Relaxation effects and the influence of the low power AFP pulses were not considered in the simulation. A bead phantom was prepared, which consisted of a 2.5 cm ID plastic tube containing a mixture of 10 μm ORGASOL polymer beads and 0.5 mM MnCl_2 dissolved in 5% agar. 3D images were acquired on a Bruker Avance-500 11.7 T micro-imaging system with a Bruker gradient coil (ID = 4 cm, gradient strength = 2.5 G/cm/A) using a ^1H birdcage transmit/receive RF probe-head (2.8 cm ID), and a modified 3D spin echo pulse sequence (MSME) incorporated with selective hermite (pulse length = 1.267 ms, BW = 2699.3 Hz) and the AFS-AFP refocusing pulses, respectively. Scan parameters: TE/TR = 14ms/1s, matrix size = 64x64x8, FOV = 4 cm, slab thickness = 8 mm, 2 dummy scans, 1 average, scan time = 8 min 32 s.

Results: Figure 1 shows the modeled flip-angle errors generated by the AFS-AFP pulse train and by the hermite refocusing pulse in the presence of significant RF frequency offsets, respectively. The magnitude of the residue z-magnetization generated by the AFS-

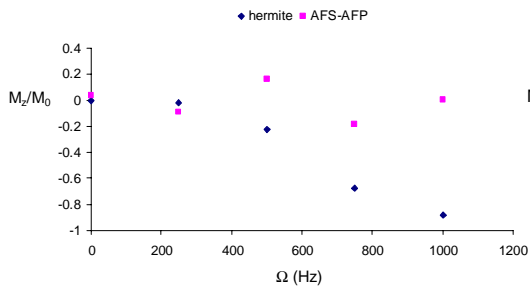


Figure 1. Residue z-magnetization (M_z/M_0) generated by hermite and AFS-AFP refocusing pulses at various RF offset (Ω).

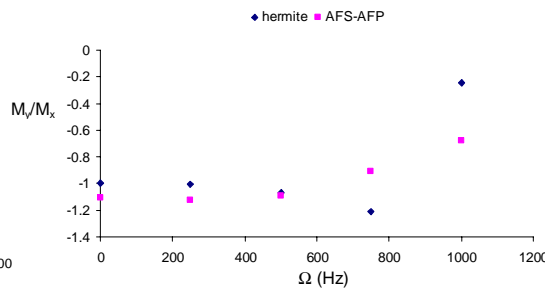


Figure 2. Transverse magnetization component ratio (M_y/M_x) after specific 180° refocusing pulses at various RF offset (Ω).

AFP pulse train is close to that of the hermite refocusing pulse at low RF offsets (Ω) and reduced significantly at high Ω -values (Fig. 1). The modeled transverse magnetization generated by the AFS-AFP pulse train is close to that of the hermite pulse at low Ω -values, and deviated much less than

those of the hermite pulse at high Ω -values (Fig. 2)

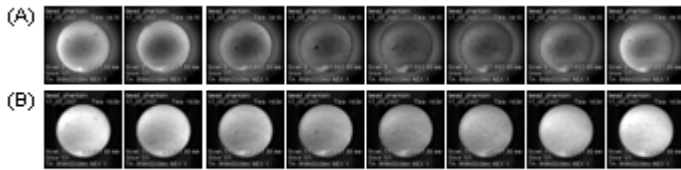


Figure 3. Axial images of the bead phantom generated by 3D MSME sequence using hermite (A) and AFS-AFP (B) pulses.

Discussion: Sample images shown in Fig. 3 demonstrate that signal sensitivity and uniformity can be substantially improved using the selective AFS-AFP pulse train. The sensitivity enhancement is ascribed to the effective compensation of the nonlinear phase dispersion and flip-angle errors by the AFS-AFP pulse train.

Reference: [1] M.S. Silver, et al, J. Magn. Reson. 59 (1984) 347-351. [2] M. Garwood, et al, J. Magn. Reson. 153 (2001) 155-177. [3] R. Bartha, et al, Magn. Reson. Med. 47 (2002) 742-750. [4] S. Michaeli, et al, Magn. Reson. Med. 53 (2005) 823-829. [5] D. Kunz, Magn. Reson. Med. 3 (1986) 377-384. [6] S. Conolly, et al, Magn. Reson. Med. 18 (1991) 28-38. [7] J.Y. Park, et al, Magn. Reson. Med. 55 (2006) 848-857.